Bioorthogonal Tetrazine Carbamate Cleavage by Highly Reactive *Trans*-Cyclooctene

Arthur H.A.M van Onzen[1], Ron M. Versteegen[2], Freek J.M. Hoeben[2], Ivo A.W. Filot[3], Raffaella Rossin[1], Tong Zhu[4], Jeremy Wu[5], Peter J. Hudson[5], Henk M. Janssen[2], Wolter ten Hoeve[6], Marc S. Robillard[1,*]

1 Tagworks Pharmaceuticals, Geert Grooteplein Zuid 10, 6525 GA Nijmegen, The Netherlands.
2 SyMO-Chem B.V., Den Dolech 2, 5612 AZ Eindhoven, The Netherlands.
3 Laboratory of Inorganic Materials Chemistry, Schuit Institute of Catalysis, Eindhoven University of Technology, P.O. Box 513, 5600 MB Eindhoven, The Netherlands
4 Levena Biopharma, 4955 Directors Place, Suite 300, San Diego, CA 92121, USA.
5 Avipep Pty Ltd, 343 Royal Parade, Parkville, VIC 3052, Australia.
6 Syncom B.V., Kadijk 3, 9747 AT Groningen, The Netherlands.

* Corresponding author. Email: marc.robillard@tagworkspharma.com

Abstract

The high reaction rate of the 'click-to-release' reaction between allylic substituted *trans*-cyclooctene and tetrazine has enabled exceptional control over chemical and biological processes. Here we report the development of a new bioorthogonal cleavage reaction based on *trans*-cyclooctene and tetrazine with up to 3 orders of magnitude higher reactivity compared to the parent reaction, and 4 to 6 orders higher than other cleavage reactions. In this new pyridazine elimination mechanism, wherein the roles a reversed, a *trans*-cyclooctene activator reacts with a tetrazine that is substituted with a methylene-linked carbamate, leading to an 1,4-elimination of the carbamate and liberation of an amine. Through a series of mechanistic studies, we identified the 2,5-dihydropyridazine tautomer as the releasing species and found factors that govern its formation and subsequent fragmentation. The bioorthogonal utility was demonstrated by the selective cleavage of a tetrazine-linked antibody-drug conjugate by *trans*-cyclooctenes, affording efficient drug liberation in plasma and cell culture. Finally, the parent and the new reaction were compared at low concentration, showing that the use of a highly reactive *trans*-cyclooctene as activator leads to a complete reaction with antibody-drug conjugate in seconds *vs*. hours for the parent system. We believe that this new reaction may allow markedly reduced click-to-release reagent doses *in vitro* and *in vivo* and could expand the application scope to conditions wherein the *trans*-cyclooctene has limited stability.

Keywords:

Bioorthogonal • Cleavage • Click Chemistry • IEDDA • Pyridazine Elimination • 1,4-elimination • Tetrazine *Trans*-Cyclooctene

Introduction

Bioorthogonal cleavage reactions have emerged as powerful strategies to control the release or activation of small molecules and biomolecules in chemical and biological settings.[1–3] Most organic cleavage reactions were derived from their click conjugation counterparts and include the reactions between tetrazines and vinyl ethers,[4–6] vinylboronic acids,[7] 3-isocyanopropyls,[8] cyclooctynes[9] and benzonorbornadienes,[10] the iminosydnone cyclooctyne reaction,[11,12] the azide-to-amine reduction by *trans*-cyclooctene (TCO),[13,14] in addition to the use of the Staudinger reaction[15,16] and ligation.[17] We reported that the fastest bioorthogonal conjugation reaction, the inverse-electron-demand Diels-Alder (IEDDA) between TCO and tetrazine derivatives,[18] widely used for selective and efficient bioconjugations *in vitro* and *in vivo*,[19,20] could be transformed into a bioorthogonal cleavage reaction.[21] In this IEDDA pyridazine elimination reaction, termed 'click-to-release' (Scheme 1A), a carbamate-linked payload is installed on the allylic position of TCO. Following reaction of the TCO-carbamate with a tetrazine, the resulting 1,4-dihydropyridazine intermediate rapidly eliminates the amine-containing payload and CO_2.

The high reactivity and selectivity of the IEDDA pyridazine elimination reaction has led to its widespread application, such as in *in vivo* cleavage or unmasking of TCO-containing antibody-drug conjugates (ADCs),[22,23] prodrugs,[24,25] proteins,[26,27] and peptide antigens,[28] by the administration of a tetrazine activator. In addition, this click-to-release approach has been used in a range of diverse *in vitro* applications, such as uncaging of fluorogenic compounds[29,30] and enzyme substrates,[31] cell-specific proteome labelling,[32] oligonucleotide delivery into cells,[33] and purification of solid phase synthesized oligonucleotides.[34]

Nevertheless, a further increase of the click-to-release reaction rate would be beneficial for a number of applications. For example, complete *in vivo* activation of a target-localized protein or ADC requires the intravenous administration of a large excess of tetrazine activator. A higher click reaction rate may allow a lower dose of the activator, which would facilitate clinical translation and may open up other prodrug approaches. Likewise, a higher reactivity would enable *in vitro* assays that use low concentrations. Here, the TCO is a limiting factor, as it has a reduced reactivity due to the allylic-positioned payload and as it needs to remain stable for hours or days when used as a linker or mask. The latter precludes increasing the reactivity by designing more strained TCO derivatives as these will likely become too unstable.[35] Furthermore, TCOs in general and highly strained TCOs in particular do not combine well with high thiol concentrations, low pH or UV light, which may affect their application scope in, for example, *in vitro* assays or chemistry.

We therefore set out to develop a new click-to-release strategy, still based on the robust IEDDA reaction between TCO and tetrazine and the unique and versatile properties of the dihydropyridazine intermediates, but now with the TCO being the activator and the tetrazine the linker. In such a system, wherein the roles are reversed, the TCO does not require the allylic substitution, and its reactivity can be boosted further as the stability requirements for the activator are less stringent than for the linker, which typically has to withstand harsher conditions and/or remain intact for a longer time. Another advantage of such a system would be that relatively simple, even commercially available, TCOs could be used. IEDDA reactions give 4,5-dihydropyridazines (DHPs), which usually rapidly tautomerize to 1,4- and 2,5-dihydropyridazines.[36,37] We envisioned that the dihydropyridazine IEDDA intermediates, of which the 1,4-dihydropyridazine leads to an electron cascade elimination of a carbamate from the part originating from the allylic position on the TCO,[21,31] may also be enlisted for an electron cascade elimination of a carbamate from the part originating from the tetrazine. Specifically, we hypothesized that a reaction of a TCO with a tetrazine substituted with a methylene-linked carbamate and subsequent tautomerization of the 4,5-dihydropyrididazine (**4,5-DHP**) to the 1,4- and 2,5- dihydropyridazines (**1,4-DHP** and **2,5-DHP**) would lead to an 1,4-elimination of the

carbamate from either **1,4-DHP** or **2,5-DHP**, or both, liberating the amine, CO_2 and pyridazine **P2** (Scheme 1B).[38]

Here we show that the dihydropyridazine product from the reaction between *trans*-cyclooctene and tetrazine can indeed be enlisted to induce an 1,4-elimination of a methylene-linked carbamate on the tetrazine. Through a series of mechanistic studies we found that **4,5-DHP** preferentially tautomerizes to **2,5-DHP** and that, fortuitously, **2,5-DHP** is the releasing species. Depending on the TCO used the reactivity increased 6- and 800-fold compared to the parent pyridazine elimination reaction, and affording release yields of 67 to 93 %. The bioorthogonality of the system was demonstrated in the context of an antibody-drug conjugate comprising the new tetrazine linker, which could be efficiently reacted and cleaved in biological conditions.

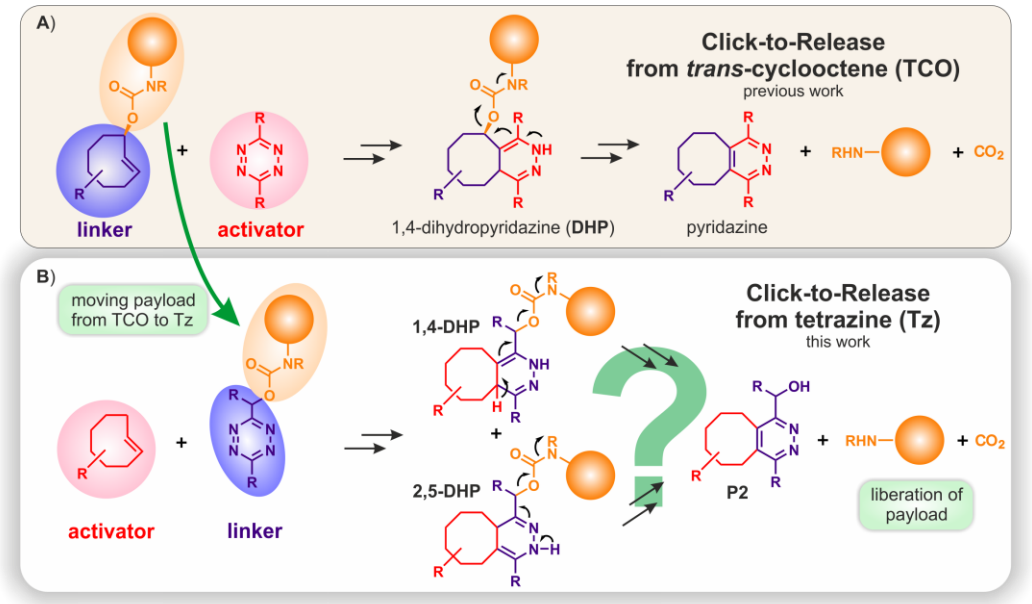

Scheme 1. A) Established click-to-release reaction with *trans*-cyclooctene as the tetrazine-cleavable linker. B) Envisioned click-to-release reaction with tetrazine as the *trans*-cyclooctene-cleavable linker.

Results and Discussion

We commenced with the preparation of a range of model 1,2,4,5-tetrazines with methylene carbamate derivatives on the 3-position, or both the 3- and 6- positions, comprising benzylic or aromatic amines with and without alkyl substituents on the amine and the methylene bridge (Figure 1A). These compounds were then screened for stability and TCO **12**-triggered carbamate cleavage in 20 % acetonitrile (ACN) / phosphate buffered saline (PBS) at 37 °C (Figure 1B,C).

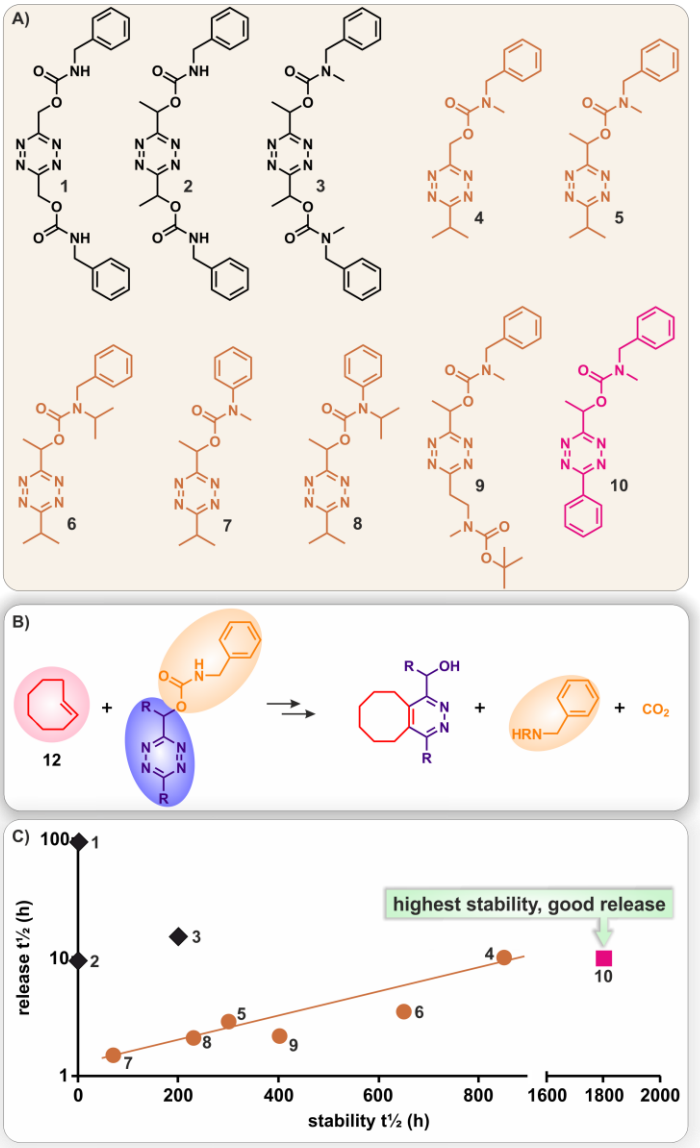

Figure 1. Stability and release study of several model tetrazine linkers. A) Structures of the evaluated model tetrazine carbamates. B) Reaction between TCO **12** and model tetrazines. C) Plot of tetrazine stability half-life *vs.* TCO **12**-triggered release half-life, in 20 % ACN/PBS, 37°C; stability determined by monitoring UV-Vis absorption at 520 nm; release measured by rapid formation of IEDDA adduct and monitoring its decrease upon carbamate elimination with LC-MS.

To our delight, already among the first three prepared compounds, symmetrical tetrazines **1**-**3**, we observed good TCO-triggered cleavage and reasonable stability for **3**. While compounds **1** and **2** showed release as well, they were highly unstable, indicating a destabilizing effect from the primary carbamate NH on the tetrazine. Based on these results, we designed non-symmetrical model compounds **4**-**10** that could form the basis of a click-cleavable linker. Perusal of Figure 1C shows triggered cleavage half-lives between 1.5 h and 10 h and a correlation between release rate and stability half-lives. Installing a methyl substituent on the methylene appears to facilitate the cleavage (**5** *vs.* **4**, and **2** *vs.* **1**). This is in line with structure activity relationships established for the widely used self-immolative *para*-aminobenzyloxycarbonyl linker wherein a methyl substituent on the methylene bridge leads to more efficient liberation due to stabilization of the increasing positive charge upon release of the carbamate.[39,40] Furthermore, benzylamine-derived tetrazine carbamates were more stable than aniline-derived carbamates (**5** *vs.* **7**, **6** *vs.* **8**) and both carbamate types could be stabilized further by replacing the N-methyl by the bulkier N-isopropyl substituent (**6** *vs.* **5**, **8** *vs.* **7**). However, comparing **5** with **9** suggests that the increased steric bulk of a branched *vs.* linear alkyl substituent on the 6-position of the tetrazine does not further improve the stability.

On the contrary, the analogous tetrazine **10** with a phenyl substituent showed a 6-fold higher stability. While this was accompanied by a slower release than the isopropyl analog **5**, we believed the enhanced stability was more important for most applications, and we continued our investigations with this tetrazine motif.

To further study the release, we prepared **11** (Figure 2A), the dimethylamine analog of **10**, and started by monitoring its TCO-triggered cleavage in a range of ACN/PBS ratios with liquid chromatography–mass spectrometry (LC-MS). To facilitate analysis, reaction mixture aliquots were rapidly oxidized to give stable mixtures of (aromatic) pyridazines **P1** and **P2** (Figure 2A), the ratio of which affording the release yield. The structure of **P2** was confirmed by reference compound synthesis (see Supporting Information), indicating that 1,4-elimination of the carbamate is followed by hydration of the exocyclic double bond of the elimination product (**EP**, Figure 2A, 2D). While the IEDDA cycloaddition between **11** and **12** was instantaneous in all mixtures, the ensuing dimethylamine elimination from the dihydropyridazine intermediate showed a strong correlation with the water content (Figure 2B). Reaction in 25 % ACN/PBS afforded dimethylamine liberation with a half-life of 20h, but in 50 % ACN/PBS, the release slowed down to a 54h half-life and, interestingly, no cleavage was observed in 100 % ACN. This trend, together with the 10h release half-life observed in 20 % ACN for the product of **10** and **12** (Figure 1C), indicated that the release half-life in fully aqueous conditions was likely to be less than 3h.

Subsequently, the reaction between **11** and **12** was studied in $CDCl_3$ with ^1H NMR, UV-Vis and IR, showing instantaneous formation of the initial 4,5-dihydropyridazine product (**4,5-DHP**) with λ-max of 279 nm as a mixture of two diastereomers (83 *vs.* 17 %), arising from the stereocenter on the methylene (Figure 2E, F, Supporting Information Section S3.2). In these conditions, **4,5-DHP** did not tautomerize further and did not release dimethylamine. Addition of 0.1 v/v% formic acid resulted in complete tautomerization[31,41] within 3h to give a mixture in a 73/27 ratio of the 2,5- and 1,4-dihydropyridazines (**2,5-DHP** and **1,4-DHP**), each present as two diastereomers, as demonstrated by the loss of peaks at 7.9 and 3.2 ppm and the appearance of 4 new sets of peaks between 6.0 and 5.4 ppm and 3.8 and 3.1 ppm (Figure 2E; see Figure S6 for 2D NMR characterization). This tautomerization was accompanied by the appearance of an IR resonance at 3340 cm^{-1} for the N-H moiety (Figure S9), and the appearance of a UV absorbance at 340 nm in addition to the band at 280 nm (Figure 2F). To understand this, the UV spectra of the three tautomers were simulated using time-dependent density functional theory (TDDFT) in conjunction with implicit solvent effects employing the COSMO model with parameters for water, leading to a predicted λ-max of 276, 290/307 and 346 nm for respectively the 4,5-, 2,5 and the 1,4-tautomer, matching the trend in the previous observations (Figure 3). Extending the incubation in acidic conditions to 184h resulted in conversion of **2,5-DHP** into **1,4-DHP**, affording a 26/74 mixture and a concomitant increase of the 340/280 nm absorbance ratio, as predicted (Figure 2E, F). Also some oxidation to the aromatic pyridazine (**P1**) occurred, similar to the previously reported pyridazine elimination reaction.[21,31] Even though all three tautomers could be formed in $CDCl_3$, no release was observed, which is possibly due to the need to stabilize the charges on the carbamate and methylene that develop upon release.[39,40] Alternatively, proton-assisted mechanisms wherein water acts as the proton carrier can be a critical pathway in the cleavage mechanism.

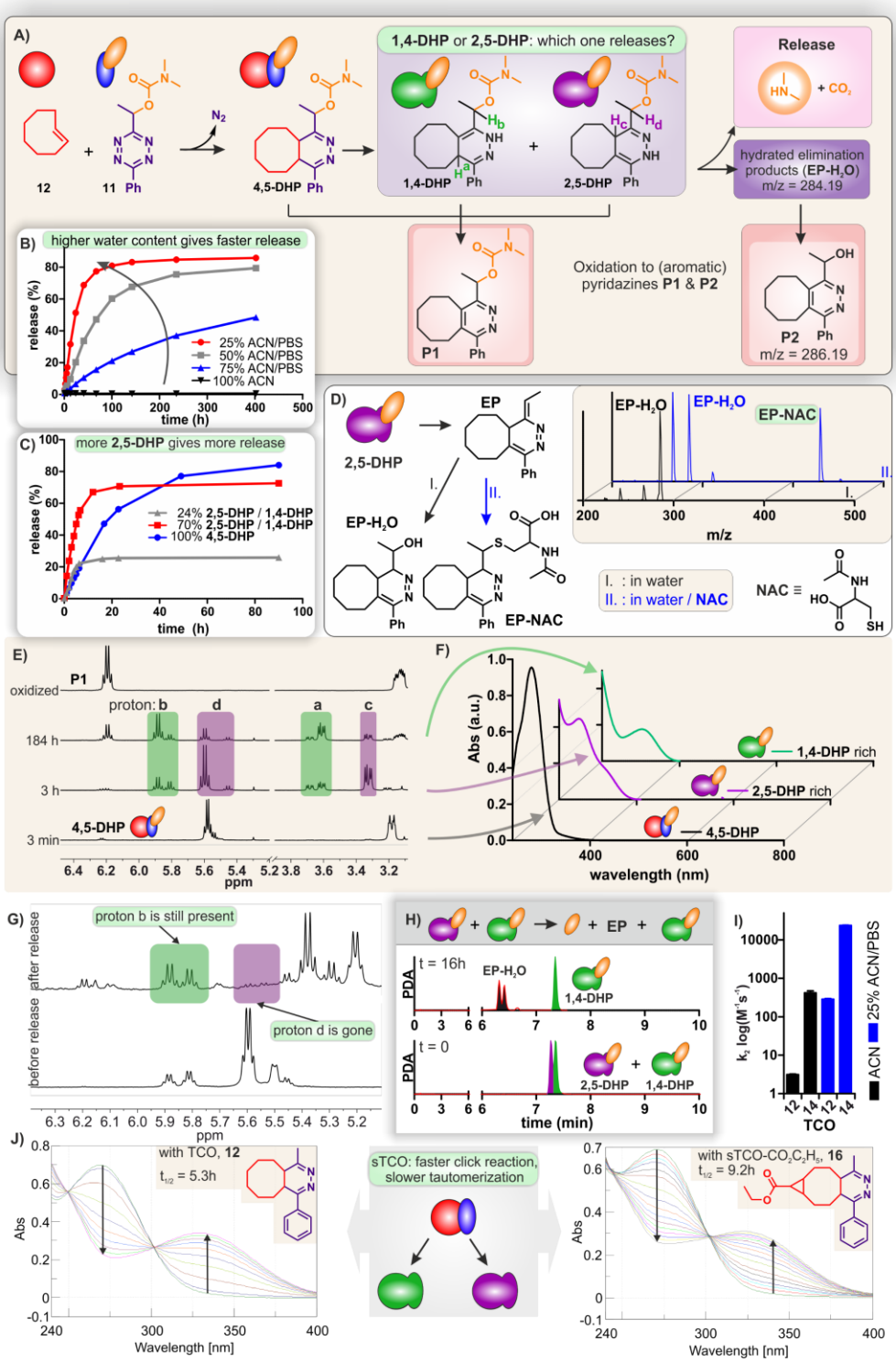

Figure 2. Mechanistic studies. A) Reaction of TCO **12** with model tetrazine **11**, affording **4,5-DHP** and then **1,4-DHP** and **2,5-DHP**, of which one liberates dimethylamine, in conjunction with hydrated elimination product (**EP-H₂O**), and oxidized pyridazines **P1** and **P2**. B) Release reaction between **11** and **12** in ACN/PBS mixtures at 37°C, quantified with LC-MS after sample oxidation to **P1**/**P2**. C) Release reaction between **11** and **12**, starting from different tautomer compositions in 25% ACN/PBS at 37°C, quantified with LC-MS after sample oxidation to **P1**/**P2**. D) Putative structure of the elimination product (**EP**), formed upon release from **2,5-DHP**, and its (I) reaction with water and (II) trapping by N-acetyl cysteine (**NAC**), as demonstrated by LC-MS. E) ^{1}H NMR of reaction of **11** with **12** in $CDCl_3$. F) UV of NMR samples of E) diluted in ACN. G) ^{1}H NMR of reaction product of **11** with **12** in $CDCl_3$ that was incubated in 25 % ACN/PBS for 3 days (top) compared to a non-incubated sample (bottom). H) PDA trace of reaction product of **11** with **12** (70/30 mixture of **2,5-/1,4-DHP**) in 25% ACN/PBS at 37°C, monitored with LC-MS of non-oxidized samples. I) Second order rate constants of the reaction of tetrazine **11** with TCOs **12** and **14** in ACN and 25% ACN/PBS at 20°C. J) UV of tautomerization of the **4,5-DHP** product from the reaction between 3-methyl-6-phenyl-tetrazine and, resp. TCO **12** and sTCO ethyl ester **16** in 25% ACN/PBS at 20°C.

The ability to control the tautomerization in chloroform was subsequently applied to identify the releasing tautomer by comparing the release profiles when starting from **4,5-DHP**, or a composition rich in respectively **2,5-DHP** or **1,4-DHP**. This was achieved by starting the reaction between **11** and **12** in $CDCl_3$ and by controlling the tautomer formation as shown above. Samples with the desired tautomer were concentrated and then dissolved in 25 % ACN/PBS, incubated at 37°C, followed by oxidation of aliquots and evaluation of the **P1/P2** ratio with LC-MS (Figure 2C). Starting from **4,5-DHP** led to a steady release of eventually 85 % with a half-life of the maximum cleavage yield of 14h, similar to when the release was started directly in 25 % ACN/PBS (Figure 2B). Interestingly, starting from a 70/30 mixture of **2,5-/1,4-DHP** afforded a much faster liberation, with a half-life of the maximum cleavage yield of 3h, leading to a maximum cleavage of 71 %. On the contrary, starting from a 24/76 mixture of **2,5-/1,4-DHP** led to a reduced maximum release yield of only 26 %. The strong correlation between the **2,5-DHP** percentage and release yield as well as the marked release rate increase when starting from **2,5-DHP** clearly indicates this is the releasing species. To confirm this, we set out to identify the non-releasing tautomer by incubating tetrazine **11** and TCO **12** in 25 % ACN/PBS at 37°C for 3 days. Given the release rate observed in these conditions (see Figure 2B) it follows that the releasing tautomer(s) would have to be consumed at that time. Indeed, subsequent lyophilization and NMR in $CDCl_3$ clearly showed that **1,4-DHP** was still present, together with some oxidized **P1**, but the signals belonging to the **2,5-DHP** had disappeared, confirming this is the releasing species (Figure 2G). In line with this and the established UV signatures of the tautomers, LC-MS of non-oxidized aliquots from of the 70/30 mixture of **2,5-/1,4-DHP** in 25 % ACN/PBS, showed the two tautomers as adjacent peaks with respectively a λ-max of 278 and 327 nm, with the 278 nm peak disappearing in time, in conjunction with the formation of hydrated elimination product (**EP-H_2O**) (Figure 2H and D). To confirm that the formation of **EP-H2O** and the corresponding **P2** is the result of 1,4-elimination followed by addition of water to the exocyclic double bond of **EP**, instead of hydrolysis of the carbamate bond of **2,5-DHP**, **11** and **12** were incubated in 25 % ACN/PBS containing the N-acetyl cysteine (NAC) to trap **EP**. As expected, LC-MS of the reaction mixture clearly showed the formation of the cysteine adduct **EP-NAC** in addition to **EP-H2O** (Figure 2D). The foregoing demonstrates that in aqueous conditions the **4,5-DHP** predominantly tautomerizes to the **2,5-DHP** and to a minor extent to the **1,4-DHP**, of which **2,5-DHP** then liberates the carbamate. Furthermore, the formation of **EP-H_2O**, **EP-NAC** and **P2** indicates that this release occurs via the envisioned 1,4-elimination.

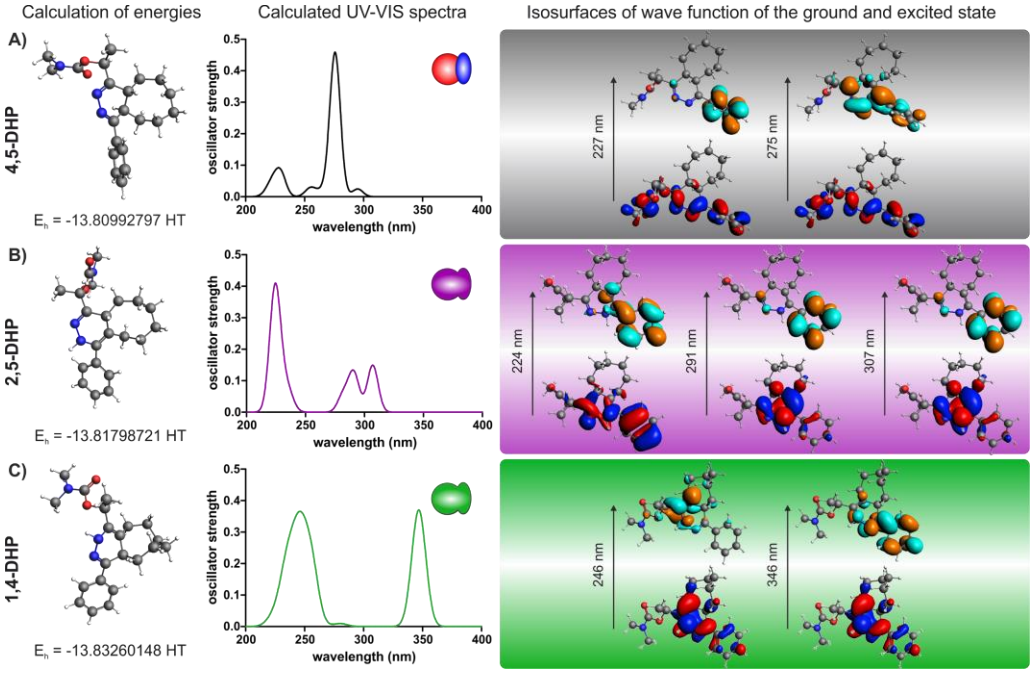

Figure 3. Simulated UV-VIS spectra of A) **4,5-DHP**; B) **2,5-DHP** and C) **1,4-DHP**. The isosurfaces of the ground and excited state corresponding to the transitions with the highest oscillator strength are shown on the right. (ground state: red and blue; excited state: teal and orange). Bonding energies of the ground states are given using water as implicit solvent.

To further support the mechanistic findings we calculated the minimal energies of **4,5-DHP**, **2,5-DHP** and **1,4-DHP** (Figure 3) and several other possible tautomers of the reaction product of **11** and **12**, including the 1,2-dihydropyridazine and its exocyclic analog (Table S1). Using a B3LYP exchange-correlation functional and water as an implicit solvent, the **2,5-DHP** and **1,4-DHP** were indeed shown to have the lowest energy, with the **1,4-DHP** being slightly lower. Calculations in vacuum showed essentially the same result, but with a slightly smaller energetic difference between the two tautomers (Table S1). These values, combined with the NMR study (Figure 2E), suggest that upon **4,5-DHP** tautomerization **2,5-DHP** is kinetically favoured and can slowly convert to the thermodynamically favoured **1,4-DHP**. The high release yield in 25 % ACN/PBS indicates that this 2,5- to 1,4-tautomerization does not readily occur in neutral aqueous conditions.

Having identified the releasing tautomer, we evaluated the potential reactivity advantage of this system. Click reaction of **11** with **12** in ACN afforded a k_2=3.14 +/- 0.10 M^{-1} s^{-1} at 20°C, which is already 6-fold faster than the parent reaction of allylic substituted TCO with 3,6-bisalkyl-tetrazine.[21] Conformationally strained TCO (sTCO) based on a *cis*-fusion of a cyclopropyl to the TCO ring represents the most reactive TCO that still has good utility in bioorthogonal conjugations.[42] Reaction of **11** with this much more reactive sTCO-acid **14** was found to have a very high k_2= 420 ± 49 $M^{-1}s^{-1}$, 800-fold higher than the parent click-to-release reaction (Figure 2I).[21] As expected, in 25 % ACN/PBS these rates increased further to 287 ± 10 M^{-1} s^{-1} for **12** and to the very high rate of 23800 ± 400 M^{-1} s^{-1} for **14**.

To demonstrate the proof of principle of this novel click-to-release reaction in a biological environment, we developed an antibody-drug conjugate (ADC) comprising the drug monomethyl auristatin E (MMAE) linked via the tetrazine to a pegylated CC49 diabody that targets tumor associated glycoprotein 72 (TAG72).[23] Based on model compound **11** we prepared tetrazine linker **18** via a modified Pinner synthesis (Figure 4A) followed by PNP carbonate formation and introduction of the MMAE. After Boc-deprotection, tetrazine-MMAE **21** was conjugated to PEG derivative **22**, affording maleimide-functionalized Tz-MMAE linker **23**. Linker-drug **23** was then site-specifically conjugated to four engineered cysteine residues in the CC49 diabody providing **tz-ADC** with a drug-to-antibody ratio (DAR) of 4 (61 kDa, Figure 4B). **Tz-ADC** exhibited excellent stock stability (PBS, 4°C) as no tetrazine degradation or spontaneous drug liberation was observed in 1 year (Figure S22). In addition to TCO **12** and sTCO-acid **14** we also prepared the DOTA chelate-conjugated analogs **13** and **15**, for increased hydrophilicity and to be able to monitor their reaction with **tz-ADC** by labeling the chelate with a radiometal (Figure 4D). The four TCOs were subsequently examined for their ability to liberate MMAE from the **tz-ADC** (Figure 4C,E-G). For all TCOs, mass spectrometry of the diabody in PBS showed efficient conversion of the ADC (30691 Da for the scFv monomer, each monomer linked to 2 MMAE) to the IEDDA product, followed by formation of species that had eliminated 1 or 2 MMAE moieties. Whereas TCO **12** and its DOTA analog **13** afforded a MMAE release yield of 93 %, the sTCO motif had a lower maximal cleavage yield of ca. 67 % (Figure 4F). Similar results were obtained in mouse plasma, while only low levels of free MMAE were found when the ADC was incubated without a TCO (Figure 4G). We hypothesized that the lower release from sTCO may be caused by a slower tautomerization of the **4,5-DHP** derivative, which may allow for more oxidative deactivation to **P1**. Indeed, when we used UV to evaluate the tautomerization of the **4,5-DHP** product from the reaction between 3-methyl-6-phenyl-tetrazine and, respectively TCO **12** and sTCO ethyl ester **16** in 25 % ACN/PBS, we found a markedly slower tautomerization for the sTCO (Figure 2J). Despite the lower overall release from sTCO-derived **2,5-DHP**, the remarkable reactivity increase offered by these TCOs provides a compelling argument for their use when the application is relatively demanding (e.g. at low concentrations). Furthermore, the cleavage yield is on par with the release observed for the widely used 3-pyrimidyl-6-methyl-tetrazine based activators[29,30] and TCO-linked ADC (data not shown).

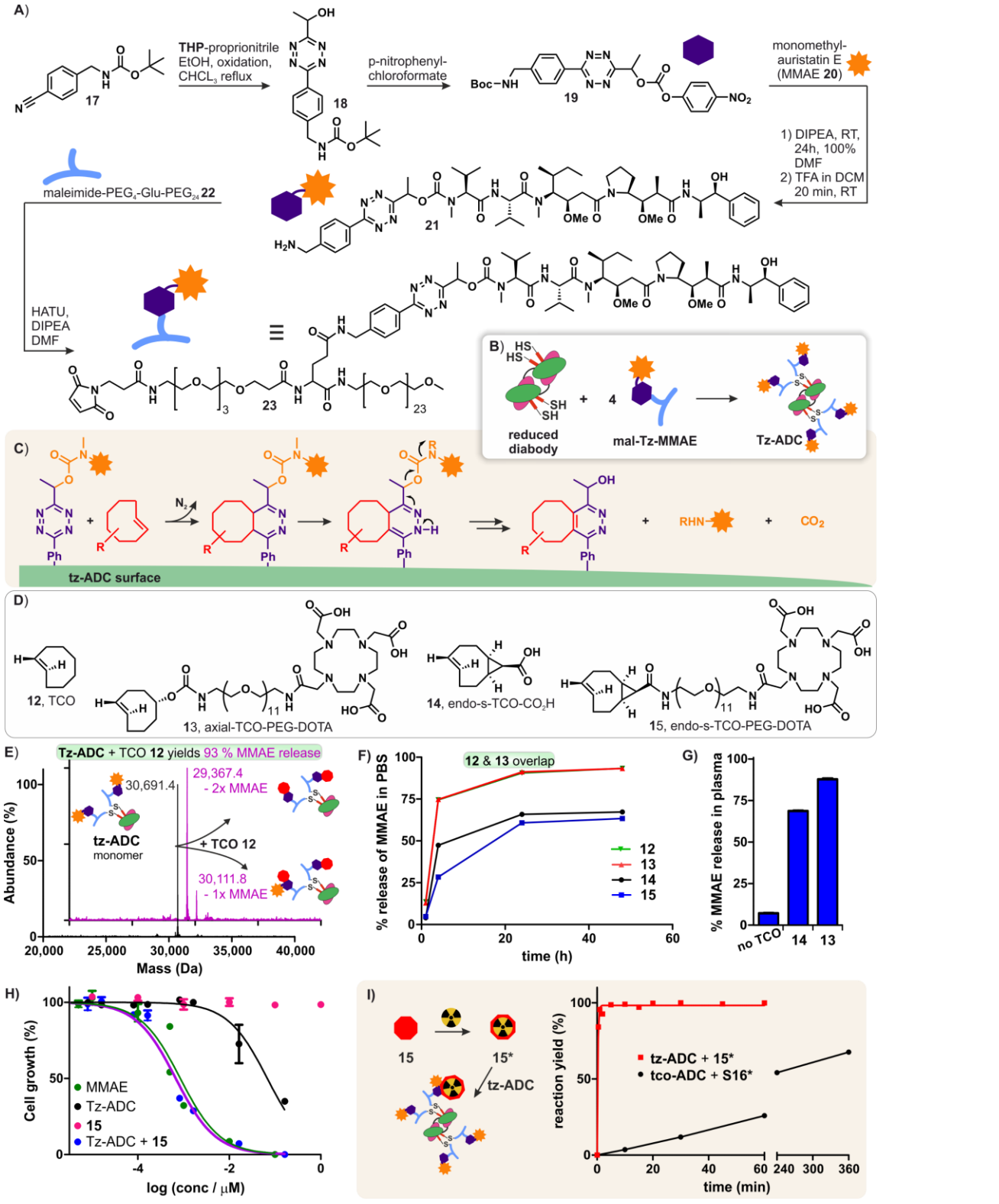

Figure 4. Evaluation of a TCO-cleavable antibody-drug conjugate. A) Synthesis of maleimide-PEG-tetrazine-MMAE **23**. B) Conjugation of **23** to diabody affording **tz-ADC**. C) TCO-triggered cleavage of MMAE from **tz-ADC**. D) Structures of TCO derivates used for release studies. E) Protein MS of **tz-ADC** (black) and of TCO **13**-activated **tz-ADC** (magenta) after 24h in PBS. F) TCO-triggered release of MMAE from **tz-ADC** in PBS. G) TCO-triggered release of MMAE from **tz-ADC** in mouse plasma after 24h quantified by LC-MS of liberated MMAE. H) Cell proliferation assay on TAG72-positive LS174T human colon carcinoma cells treated with **tz-ADC** alone or in combination with activator **15**, **15** alone or free MMAE; data are the mean with s.e.m (n=3); I) Schematic representation of radiolabelling of TCO **15** with 111-indium, resulting in **15***, which was reacted with **tz-ADC** in PBS at 37°C at 0.15 equivalents with respect to the diabody (0.6 μM); similarly **tco-ADC** (0.6 μM) was reacted with 0.36 equivalents of radiolabelled tetrazine **S16**.

ADCs allow the safe and effective use of highly potent drugs like MMAE, which are too toxic to be used as free drugs. After ADC targeting of the cancer cell, these drugs typically need to be cleaved from their antibody linker to exert their therapeutic effect. As a proof of principle of the TCO-cleavable **tz-ADC** we evaluated the cytotoxicity of **tz-ADC** and TCO **15** alone and in combination in a human colorectal cancer cell culture. TCO **15** alone was not toxic while **tz-ADC** alone only exhibited a relatively moderate activity (Figure 4H). However, when a fixed dose of 3.3 µM of TCO **15** was combined with the **tz-ADC,** the cytotoxicity increased 100-fold, affording an EC50 value of 0.67 nM, matching the toxicity of the parent drug MMAE, clearly underlining the efficacy of this new cleavage system. Finally, to demonstrate the reactivity advance offered by click-to-release from tetrazine *vs.* click-to-release from TCO, we compared the click reaction between a previously reported TCO-linked MMAE diabody ADC (**tco-ADC**)[23] and ^{177}Lu-labelled DOTA-tetrazine activator (**S16**) with the reaction of **tz-ADC** with ^{111}In-labelled DOTA-sTCO **15** in PBS at 37°C at a very low concentration of 0.6 µM in nearly equimolar conditions. Figure 4I shows the striking difference between the two systems, with the conjugation of **15** complete within 1 minute, while the conjugation of the tetrazine activator had a 3h half-life.

Conclusion

We have developed a new and highly reactive bioorthogonal elimination reaction that enables traceless release of an amine-containing payload from a tetrazine following reaction with a *trans*-cyclooctene. This was achieved by switching the roles of the tetrazine and TCO in the parent IEDDA pyridazine elimination, now permitting the use of highly reactive sTCO derivatives as activators, boosting the reactivity 3 orders of magnitude compared to the parent click-to-release reaction, and 4 to 6 orders of magnitude compared to the other known cleavage reactions.[4-17] Even the non-conformationally strained TCOs already gives 6-fold higher reactivity than the parent reaction combined with near quantitative release yields. Through mechanistic studies we demonstrated that the releasing tautomer is the 2,5-dihydropyridazine, which fortuitously is the favoured IEDDA product, and we found that the formation rate of this species is dependent on the type of TCO being used. By trapping the elimination product, we could show that the release occurs via the hypothesized 1,4-elimination. Furthermore, the strong dependence on water indicates a direct role for water in the electron cascade elimination mechanism. The new click-cleavable linker was subsequently applied in an ADC, which exhibited TCO-triggered drug cleavage half-lives down to 2h in fully aqueous conditions and showed good controlled release in biological conditions in plasma and in cell culture. Activation of the ADC led to effective cancer cell killing with the same potency as the free drug. Furthermore, a head-to-head comparison of the click reaction of TCO-linked ADC with radiolabelled tetrazine and tetrazine-linked ADC with radiolabelled TCO at very low concentration, underlined the pronounced advance offered by the highly reactive TCO-triggered dihydropyridazine elimination, for example for cases when the activator cannot be used in large excess.

These results hold promise for *in vivo* drug release and unmasking applications, potentially allowing substantially reduced activator doses. We also envision the use of this reaction in chemical biology, life-science assays, and material chemistry, enabling the controlled (dis)assembly of molecules, proteins, cells, or biomaterials at low concentration or in conditions that are incompatible with the TCO. For example, contrary to TCOs, tetrazines are typically stable at low pH. While the click-to-release from TCO offers faster release kinetics, we expect that the versatile click-to-release from tetrazine harbours ample opportunity for further improvements in cleavage rate and yield. Finally, the presented release chemistry can be performed with commercially available TCOs and uses tetrazine linkers and masks that are easier to prepare than TCO linkers, making highly reactive click-to-release chemistry available to a larger research community.

Acknowledgements

We thank Kim Bonger (Radboud University, Nijmegen) for critical reading of the manuscript. We gratefully acknowledge the support of the European Regional Development Fund (EFRO), Operation Program Oost, for Project "Proeftuin Nanomedicine".

References

1. Li, J. & Chen, P. R. Development and application of bond cleavage reactions in bioorthogonal chemistry. *Nat. Chem. Biol.* **12**, 129–137 (2016).
2. Tu, J., Xu, M. & Franzini, R. M. Dissociative Bioorthogonal Reactions. *ChemBioChem* **20**, 1615–1627 (2019).
3. Sabatino, V., Rebelein, J. G. & Ward, T. R. “Close-to-Release”: Spontaneous Bioorthogonal Uncaging Resulting from Ring-Closing Metathesis. *J. Am. Chem. Soc.* **141**, 17048–17052 (2019).
4. Jiménez-Moreno, E. *et al.* Vinyl Ether/Tetrazine Pair for the Traceless Release of Alcohols in Cells. *Angew. Chem. Int. Ed.* **56**, 243–247 (2017).
5. Neumann, K. *et al.* Tetrazine-Responsive Self-immolative Linkers. *ChemBioChem* **18**, 91–95 (2017).
6. Wu, H., Alexander, S. C., Jin, S. & Devaraj, N. K. A Bioorthogonal Near-Infrared Fluorogenic Probe for mRNA Detection. *J. Am. Chem. Soc.* **138**, 11429–11432 (2016).
7. Lelieveldt, L. P. W. M., Eising, S., Wijen, A. & Bonger, K. M. Vinylboronic acid-caged prodrug activation using click-to-release tetrazine ligation. *Org. Biomol. Chem.* **17**, 8816–8821 (2019).
8. Tu, J., Xu, M., Parvez, S., Peterson, R. T. & Franzini, R. M. Bioorthogonal Removal of 3-Isocyanopropyl Groups Enables the Controlled Release of Fluorophores and Drugs in Vivo. *J. Am. Chem. Soc.* **140**, 8410–8414 (2018).
9. Zheng, Y. *et al.* Enrichment-triggered Prodrug Activation Demonstrated through Mitochondria-targeted Delivery of Doxorubicin and Carbon Monoxide. *Nat. Chem.* **10**, 787–794 (2018).
10. Xu, M., Galindo-Murillo, R., Cheatham, T. E. & Franzini, R. M. Dissociative reactions of benzonorbornadienes with tetrazines: scope of leaving groups and mechanistic insights. *Org. Biomol. Chem.* **15**, 9855–9865 (2017).
11. Bernard, S. *et al.* Bioorthogonal Click and Release Reaction of Iminosydnones with Cycloalkynes. *Angew. Chem. Int. Ed Engl.* **56**, 15612–15616 (2017).
12. Riomet, M. *et al.* Design and Synthesis of Iminosydnones for Fast Click and Release Reactions with Cycloalkynes. *Chem. Eur. J.* **24**, 8535–8541 (2018).
13. Matikonda, S. S. *et al.* Bioorthogonal prodrug activation driven by a strain-promoted 1,3-dipolar cycloaddition. *Chem. Sci.* **6**, 1212–1218 (2015).
14. Matikonda, S. S. *et al.* Mechanistic Evaluation of Bioorthogonal Decaging with trans-Cyclooctene: The Effect of Fluorine Substituents on Aryl Azide Reactivity and Decaging from the 1,2,3-Triazoline. *Bioconjug. Chem.* **29**, 324–334 (2018).
15. Luo, J., Liu, Q., Morihiro, K. & Deiters, A. Small Molecule Control of Protein Function through Staudinger Reduction. *Nat. Chem.* **8**, 1027–1034 (2016).
16. van Brakel, R., Vulders, R. C. M., Bokdam, R. J., Grüll, H. & Robillard, M. S. A doxorubicin prodrug activated by the staudinger reaction. *Bioconjug. Chem.* **19**, 714–718 (2008).
17. Azoulay, M., Tuffin, G., Sallem, W. & Florent, J.-C. A new drug-release method using the Staudinger ligation. *Bioorg. Med. Chem. Lett.* **16**, 3147–3149 (2006).

18. Blackman, M. L., Royzen, M. & Fox, J. M. Tetrazine Ligation: Fast Bioconjugation Based on Inverse-Electron-Demand Diels−Alder Reactivity. *J. Am. Chem. Soc.* **130**, 13518–13519 (2008).

19. Oliveira, B. L., Guo, Z. & Bernardes, G. J. L. Inverse electron demand Diels–Alder reactions in chemical biology. *Chem. Soc. Rev.* **46**, 4895–4950 (2017).

20. Rossin, R. *et al.* In Vivo Chemistry for Pretargeted Tumor Imaging in Live Mice. *Angew. Chem. Int. Ed.* **49**, 3375–3378 (2010).

21. Versteegen, R. M., Rossin, R., ten Hoeve, W., Janssen, H. M. & Robillard, M. S. Click to Release: Instantaneous Doxorubicin Elimination upon Tetrazine Ligation. *Angew. Chem. Int. Ed.* **52**, 14112–14116 (2013).

22. Rossin, R. *et al.* Triggered Drug Release from an Antibody–Drug Conjugate Using Fast "Click-to-Release" Chemistry in Mice. *Bioconjug. Chem.* **27**, 1697–1706 (2016).

23. Rossin, R. *et al.* Chemically triggered drug release from an antibody-drug conjugate leads to potent antitumour activity in mice. *Nat. Commun.* **9**, 1484 (2018).

24. Czuban, M. *et al.* Bio-Orthogonal Chemistry and Reloadable Biomaterial Enable Local Activation of Antibiotic Prodrugs and Enhance Treatments against Staphylococcus aureus Infections. *ACS Cent. Sci.* **4**, 1624–1632 (2018).

25. Yao, Q. *et al.* Synergistic enzymatic and bioorthogonal reactions for selective prodrug activation in living systems. *Nat. Commun.* **9**, 5032 (2018).

26. Li, J., Jia, S. & Chen, P. R. Diels-Alder reaction-triggered bioorthogonal protein decaging in living cells. *Nat. Chem. Biol.* **10**, 1003–1005 (2014).

27. Zhang, G. *et al.* Bioorthogonal Chemical Activation of Kinases in Living Systems. *ACS Cent. Sci.* **2**, 325–331 (2016).

28. van der Gracht, A. M. F. *et al.* Chemical Control over T-Cell Activation in Vivo Using Deprotection of trans-Cyclooctene-Modified Epitopes. *ACS Chem. Biol.* **13**, 1569–1576 (2018).

29. Fan, X. *et al.* Optimized Tetrazine Derivatives for Rapid Bioorthogonal Decaging in Living Cells. *Angew. Chem. Int. Ed.* **55**, 14046–14050 (2016).

30. Sarris, A. J. C. *et al.* Fast and pH-Independent Elimination of trans-Cyclooctene by Using Aminoethyl-Functionalized Tetrazines. *Chem. Eur. J.* **24**, 18075–18081 (2018).

31. Versteegen, R. M. *et al.* Click-to-Release from trans-Cyclooctenes: Mechanistic Insights and Expansion of Scope from Established Carbamate to Remarkable Ether Cleavage. *Angew. Chem. Int. Ed.* **57**, 10494–10499 (2018).

32. Du, S. *et al.* Cell type-selective imaging and profiling of newly synthesized proteomes by using puromycin analogues. *Chem. Commun.* **53**, 8443–8446 (2017).

33. Khan, I., Seebald, L. M., Robertson, N. M., Yigit, M. V. & Royzen, M. Controlled in-cell activation of RNA therapeutics using bond-cleaving bio-orthogonal chemistry. *Chem. Sci.* **8**, 5705–5712 (2017).

34. Agustin, E. *et al.* A fast click–slow release strategy towards the HPLC-free synthesis of RNA. *Chem. Commun.* **52**, 1405–1408 (2016).

35. Rossin, R. *et al.* Highly Reactive trans-Cyclooctene Tags with Improved Stability for Diels–Alder Chemistry in Living Systems. *Bioconjug. Chem.* **24**, 1210–1217 (2013).

36. Stanovnik, B., Tišler, M., Katritxky, A. R. & Denisko, O. V. The Tautomerism of Heterocycles. Six-Membered Heterocycles: Part 1, Annular Tautomerism. in *Advances in Heterocyclic Chemistry* (ed. Katritzky, A. R.) vol. 81 253–303 (Academic Press, 2001).

37. Sauer, J. *et al.* 1,2,4,5-Tetrazine: Synthesis and Reactivity in [4+2] Cycloadditions. *Eur. J. Org. Chem.* **1998**, 2885–2896 (1998).

38. Upon completion of this manuscript, Tu *et al.* reported the efficient removal of tetrazylmethyl by isonitriles compared to other dienophiles. Tu, J. *et al.* Isonitrile-responsive and bioorthogonally removable tetrazine protecting groups. *Chem. Sci.* (2020) doi:10.1039/C9SC04649F

39. Alouane, A., Labruère, R., Le Saux, T., Schmidt, F. & Jullien, L. Self-Immolative Spacers: Kinetic Aspects, Structure–Property Relationships, and Applications. *Angew. Chem. Int. Ed.* **54**, 7492–7509 (2015).

40. Hay, M. P., Sykes, B. M., Denny, W. A. & O'Connor, C. J. Substituent effects on the kinetics of reductively-initiated fragmentation of nitrobenzyl carbamates designed as triggers for bioreductive prodrugs. *J. Chem. Soc. Perkin 1* 2759–2770 (1999).

41. Carlson, J. C. T., Mikula, H. & Weissleder, R. Unraveling Tetrazine-Triggered Bioorthogonal Elimination Enables Chemical Tools for Ultrafast Release and Universal Cleavage. *J. Am. Chem. Soc.* **140**, 3603–3612 (2018).

42. Taylor, M. T., Blackman, M. L., Dmitrenko, O. & Fox, J. M. Design and Synthesis of Highly Reactive Dienophiles for the Tetrazine–trans-Cyclooctene Ligation. *J. Am. Chem. Soc.* **133**, 9646–9649 (2011).